Pergamon

Int. J. Heat Mass Transfer. Vol. 37, No. 5, pp. 737–746, 1994

0017–9310/94 $6.00 + 0.00

Models for the heat transfers during the transformations inside an emulsion—I. Crystallizations of the undercooled droplets

J. P. DUMAS, M. KRICHI, M. STRUB and Y. ZERAOULI

Laboratoire de Thermodynamique et Energétique, Université de Pau et des Pays de l'Adour, Avenue de l'Université, 64000 Pau, France

(*Received* 24 *March* 1993 *and in final form* 6 *October* 1993)

Abstract—Experiments on heat transfers inside an emulsion when the dispersed phase crystallizes or melts have previously been presented [Dumas *et al.*, *Eurotherm Seminar 5* (1988)]. The crystallization and melting processes are not symmetrical because of the large undercooling induced by the smallness of the emulsion droplet sizes. The space–time evolution of the temperature inside a metallic cylinder filled with the emulsion is investigated. The dispersed substances are either hexadecane, octadecane or water. In Part I of this paper we describe the results obtained during a steady cooling. We observe that, largely below the melting temperature, a stabilization of the temperature occurs in the axis region during a lapse of time depending on the cooling rate, the mass fraction or the final temperature. A simplified model based on a combination of the energy equation and the nucleation theories is proposed and explains the main experimental features.

1. INTRODUCTION

WE HAVE already presented experimental results on the heat transfers inside an emulsion during the crystallization or the melting of the dispersed droplets [1, 2]. The two processes are not symmetrical because of the large undercooling induced by the smallness of the emulsion droplets sizes. At the crystallization the release of energy, for a droplet, is practically instantaneous because it occurs far from the thermodynamic equilibrium but, at the melting, the absorption of energy is at the fixed melting temperature and its kinetics depends on the exchanges with the surrounding medium.

In this Part I, we present a model and its comparison to the experimental results for the determination of the heat transfers and the kinetics of the transformations upon cooling during the crystallizations of the undercooled droplets. The model and the experimental results for the melting of the droplets upon heating will be presented in Part II.

2. PHASES TRANSFORMS OF PURE SUBSTANCES

Except for some rare cases [3], the phases transforms for condensed substances take place, upon heating, at the phase equilibrium temperature without delay. So, crystals always melt at their melting temperature T_F. But, upon cooling, it is observed that the crystallizations occur at a temperature T lower than T_F. It is the undercooling phenomenon.

It is well stated that, upon cooling, the undercooling ΔT, defined as $T_F - T$, increases when the sample size decreases. For example, for water ΔT is 14 K for macrosamples a few cm^3 in volume and ΔT is 38 K for microsamples a few μm^3 in volume as for the droplets of an emulsion. Very important ΔT have been observed with organic compounds (sometimes $\Delta T \geqslant 100$ K [3]) or metals (in certain cases $\Delta T > 200$ K [4]). The undercooling can be reduced by addition of nucleation catalysts even inside the droplets of an emulsion [5, 6], but ΔT is reduced and not canceled. For example, the use of AgI with water reduces ΔT to 22 K instead of 38 K.

We must add that, for certain substances, at the crystallization of the dispersed undercooled liquid, we have observed the appearance of metastable crystalline phases and a new polymorphism has been found [3]. Finally, the vitrification of the dispersed liquid can be observed instead of its crystallization.

The main feature of crystallization is its stochastic character, i.e. samples which are apparently identical will not transform at the same temperature during the cooling process. Previous calorimetric experiments have shown that when a great number of samples is investigated (and it is the case with the emulsion which contains 10^8–10^9 droplets per mm^3) the crystallizations successively occur, upon a steady cooling, in a temperature range far below T_F and are the most numerous at a temperature T^* called the most probable temperature. It is also possible to maintain the temperature lower than T_F; in this case the crystallizations successively occur in a large lapse of time [7].

Nucleation theories (i.e. see ref. [8]) explain that inside the liquid the fluctuations create small aggregates which initiate the crystallization if they have a size greater than a critical value depending on the temperature. In fact the critical value is different if

NOMENCLATURE

a	diffusivity of the emulsion [$m^2 s^{-1}$]
Bi^{ext}	Biot number of the cell
c	specific heat of the emulsion [$J K^{-1} kg^{-1}$]
c_L or c_S	specific heat when the droplets of the emulsion are liquid or solid [$J K^{-1} kg^{-1}$]
h_{SL}	specific latent heat of fusion (> 0) [$J kg^{-1}$]
h^{ext}	external exchange coefficient for the cell [$W m^{-2} s^{-1}$]
$J_i(T)$	homogeneous or heterogeneous nucleation rate [$m^{-3} s^{-1}$]
$\mathcal{J}(T)$	probability of crystallization of one droplet per unit time [s^{-1}]
$\mathcal{J}'(\theta)$	nondimensionless probability of crystallization of one droplet
k	heat conductivity of the emulsion [$W m^{-1} K^{-1}$]
k_L or k_S	heat conductivity when the droplets of the emulsion are liquid or solid [$W m^{-1} K^{-1}$]
M	number of intervals in the grid
$n(r, t)$	number of crystallized droplets per unit volume [m^{-3}]
n_t	total number of droplets per unit volume [m^{-3}]
P	mass fraction of the dispersed substance
$\dot{q}$	heat source [$J m^{-3} s^{-1}$]
r	radius [m]
$\bar{r}$	dimensionless radius
R_0	inner radius of the cylinder [m]
S	mean area of a droplet [m^{-2}]
Ste	Stefan number of the emulsion
t	time [h]
$\bar{t}$	dimensionless time
$T(r, t)$	temperature at r and t [°C]
T_F	melting temperature [°C]
T^{**}	temperature of the plateau for the axis [°C]
T_i	final temperature after the steady cooling [°C]
$T_{\infty}(t)$	programmed temperature of the bath [°C]
T_0	initial temperature [°C]
T_r	reference temperature [°C]
T_m^i	temperature of the node m at time i [°C]
V	mean volume of a droplet [m^{-3}].

Greek symbols

β	cooling rate (< 0) [°C h^{-1}]
β'	dimensionless cooling rate
θ	dimensionless temperature
θ_i	final dimensionless temperature
$\theta_{\infty}(\bar{t})$	dimensionless temperature of the bath
ρ	mass density of the emulsion [$kg m^{-3}$]
ρ_0	mass density of the dispersed phase [$kg m^{-3}$]
τ	duration of the plateau for the axis [h]
ϕ_m^i	local proportion of the crystallized droplets for the mode m at time i
$\phi(r, t)$	local proportion of the crystallized droplets
∇	gradient or divergence operator.

the aggregate forms inside the liquid (homogeneous nucleation) or on the surface of solid particles as nucleating agents or simply the interface of the liquid with their container (heterogeneous nucleation). So, it is theoretically confirmed that when the heterogeneous nucleation is concerned the crystallization occurs at a higher temperature.

The erratic character due to the fluctuations means that it is only possible to determine either $J_{hom}(T)$, called the homogeneous nucleation rate, the probability of transformation per unit time and unit sample volume in case of homogeneous nucleation or $J_{het}(T)$, called the heterogeneous nucleation rate the probability of transformation per unit time and unit 'active' surface in case of heterogeneous nucleation.

We have [8]:

$$J_i(T) = K(T) \exp(-E/kT) \times \exp(\alpha_i/T(T_F - T)^2) i = \text{hom or het} \quad (1)$$

where $K(T)$ is a function slightly dependent on the temperature, E is an energy barrier depending on the viscosity of the liquid ($J_i(T)$ is smaller if the viscosity is higher) and α_i a constant ($\alpha_{hom} > \alpha_{het}$).

For the liquids presented here, the variation of the term $\exp(\alpha_i/T(T_F - T)^2)$ is preponderant. So, when the temperature decreases from T_F, $J_i(T)$ is practically zero down to a given temperature, and increases very sharply afterwards.

The probability of crystallization of a droplet per unit time is $J_{hom}(T)V$, where V is the droplet volume, in the case of a homogeneous nucleation or $J_{het}(T)S$, where S is the 'active' interface in the case of heterogeneous nucleation. But, even in the case of the most important undercoolings, it is impossible to state if the nucleation is homogeneous or heterogeneous [3, 7]. Moreover, the droplets have slightly different volumes or different 'active' interfaces. So, we are only able to determine experimentally $\mathcal{J}(T)$, the mean probability per unit time of crystallization of a droplet

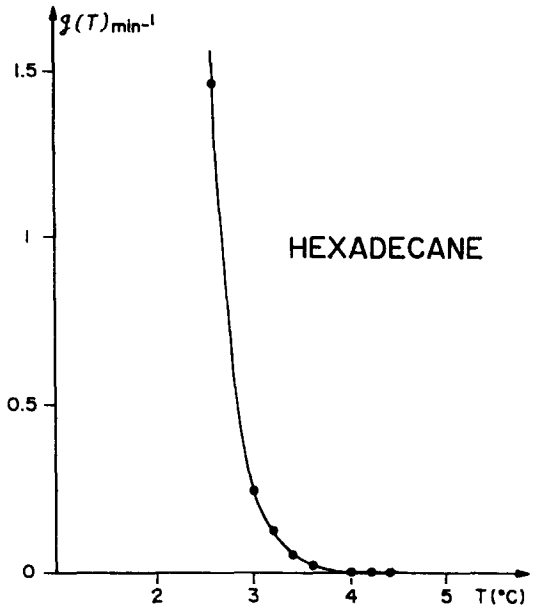

FIG. 1. Experimental curve of the crystallization probability per unit time $\mathcal{J}(T)$ for hexadecane.

which represents the mean values either of $J_{hom}(T)V$ or $J_{het}(T)S$. In Fig. 1 we see the example of $\mathcal{J}(T)$ determined by Differential Scanning Calorimetry for hexadecane [9].

3. EXPERIMENTAL

The investigated substances are Analytic Grade paraffins such as hexadecane ($T_F = 18.0°C$) or octadecane ($T_F = 27.5°C$) and distilled water. They are dispersed by a high speed stirrer within an emulsifying medium made of a mixture of water, glycerol and Tween 80® as surfactant for the paraffins and a mixture of paraffin oil and lanolin for water. For hexadecane, by a particular choice of the relative concentrations of the constitutive substances of the emulsifying medium, the dispersed system is, in fact, a microemulsion [9]. So, it is very stable and the experiments are easier. The droplet diameters are monodisperse about 10 nm. But, even in this case we will name all the dispersed systems emulsions.

The experimental cell has been presented in detail elsewhere [1, 2]. It is a vertical metallic tube (see Fig. 2(a)) of about 500 cm^3 in volume closed by two isolated caps. Its height is sufficiently larger than its diameter to consider that only the radius r and the time t are the variables of the study. This cylinder contains a 'cage' which supports 12 thermocouples tied up on stretched nylon threads. The solders are located regularly (see Fig. 2(b)) in a median horizontal plane at different radii. The cell is immersed in a bath at temperature $T_\infty(t)$ heated or cooled at a constant rate β by a thermostat.

The solders diameters ($\leqslant 1$ mm) are very much larger than the droplets diameters; so, the emulsion can be considered as an homogeneous medium. At the crystallization, which is very quick, we are not able to analyse what actually happens inside a droplet where the temperature variation is probably considerable. We have detected a global effect in a region which is small in comparison with the cell dimensions, but which could contain a great number of droplets (as

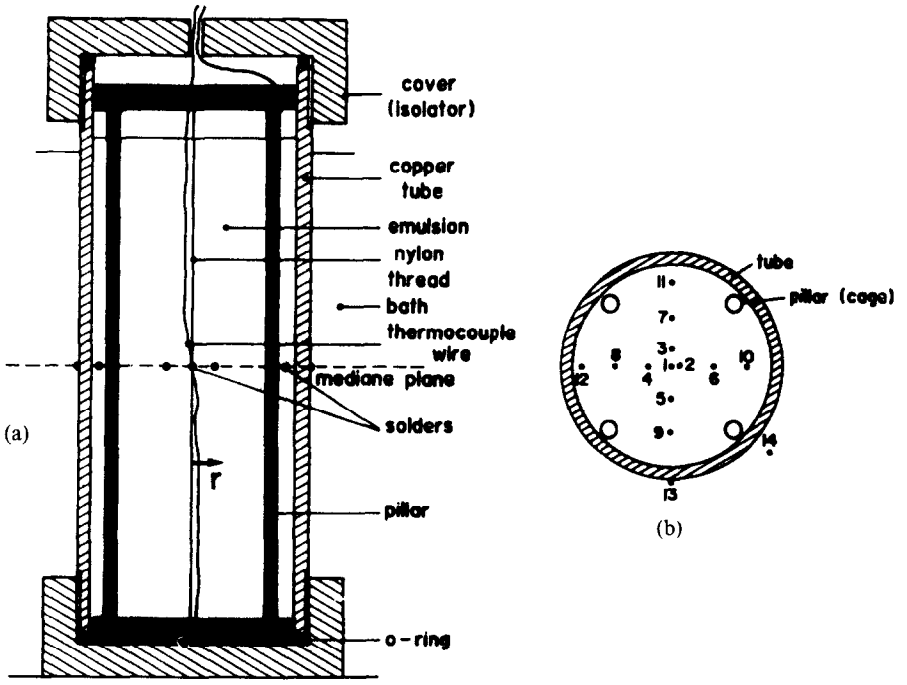

FIG. 2. Scheme of the experimental cell.

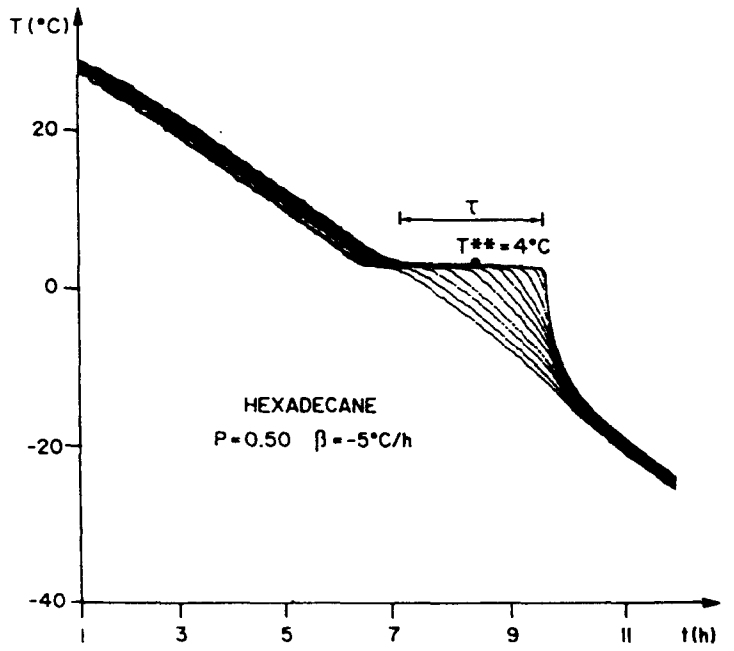

FIG. 3. Temperatures of the solders vs time for a hexadecane emulsion cooled at $\beta = -5°C\ h^{-1}$.

already mentioned there are about 10^8–10^9 droplets per mm^3).

An example of the experimental curves of the temperature of the solders vs time is given in Fig. 3 for the microemulsion of hexadecane and in Figs. 4 and 5 for the emulsions of octadecane and water. For all substances, we observe at the beginning of the cooling, before the crystallizations, the difference of the temperatures for the different radii due to the heat conduction inside the emulsion (the temperature for the axis region $r = 0$ being always the highest). Crystallizations are detected when the curves deviate from linearity.

As expected, the droplets near the inner side of the tube first crystallize; but a part of the released energy heats up the axis region of the cylinder delaying the crystallizations of the droplets. Generally, the result is that the temperature near the axis is practically

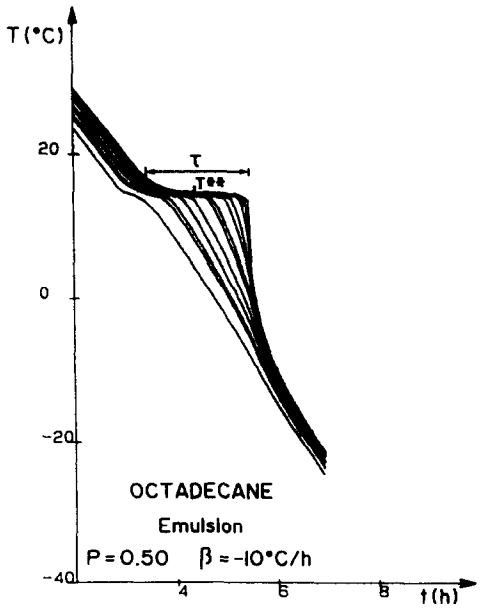

FIG. 4. Temperatures of the solders vs time for an octadecane emulsion cooled at $\beta = -10°C\ h^{-1}$.

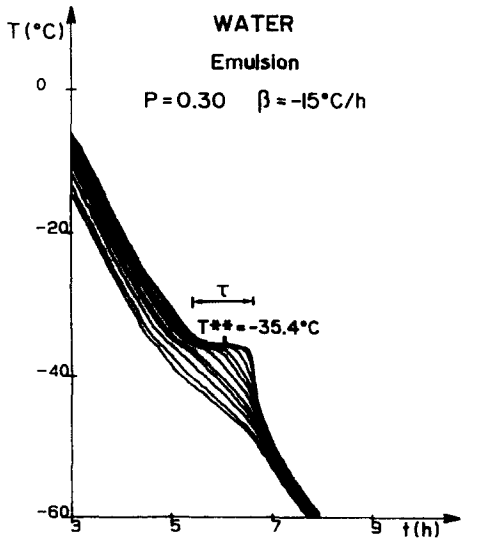

FIG. 5. Temperatures of the solders vs time for a water emulsion cooled at $\beta = -15°C\ h^{-1}$.

Table 1.

Substance	T_F	T^{**}
Hexadecane	18.0	4.0
Octadecane	27.5	14.5
Water	0.0	−35.4

constant over a lapse of time τ. Let us notice that the temperature being much lower than the melting temperature T_F, no thermodynamic reason can explain this fact.

This quasi steady temperature named T^{**} and taken for $\tau/2$ (see Figs. 3–5) varies very little, for a given substance, with the different emulsions and the different parameters we have studied. On the contrary, τ depends on these parameters as we will see later.

On Table 1 we give the mean values of T^{**} (in °C) for the three investigated substances knowing that the variation with the different parameters is smaller than 1°C.

4. ANALYSIS

In this paper we propose a model for the cooling and the crystallizations of the undercooled droplets. We present the model in the case of an emulsion in a cylinder having a height much larger than its diameter as for the experimental cell described above where only the variables r and t are taken into account.

The droplets of the emulsion are so small ($\leqslant 1\ \mu m^3$ in volume), the dispersed system is so viscous (the dynamic viscosity is larger than 10^4 cP around the crystallization temperature) and the variation of the density ρ is so small ($<1\%$ as indicated by thermo-mechanical experiments), that the possible convective diffusion inside the droplets during the change of state, does not involve a movement of the emulsion as a whole. So, only the conduction must be taken into account.

Hence, we use the energy equation:

$$\rho c \frac{\partial T(r,t)}{\partial t} = \nabla(k \nabla T(r,t)) + \dot{q} \tag{2}$$

where k is the thermal conductivity of the emulsion, ρ its mass density and c its specific heat. The heat source $\dot{q}$ is different from zero when the crystallizations of the undercooled droplets occur.

As mentioned above, we assume the homogeneity of the emulsion since the relatively large size of the thermocouples solders does not permit a more accurate investigation. Therefore, we assume, for the model, that the droplets release instantaneously the same amount of heat as a volume, V, of liquid.

The volumetric heat source, $\dot{q}$, is proportional to the heat of transformation of one droplet and to the number of droplets which crystallize per unit time and unit emulsion volume dn/dt. We have:

$$\dot{q} = \rho_0 V h_{SL}\, dn/dt \tag{3}$$

where ρ_0 is the mass density of the dispersed phase (hexadecane) and h_{SL} the latent heat of fusion ($h_{SL} > 0$).

dn/dt, the number of droplets crystallizing per unit time, is proportional to the probability of crystallization of a droplet and to the number of droplets which remain unfrozen. If an emulsion unit volume contains n_t droplets, assuming that the number of droplets crystallized at the time t per emulsion unit volume is $n(r, t)$, dn/dt is given by:

$$dn/dt = \mathcal{J}(T)(n_t - n(r,t)). \tag{4}$$

If we define $\phi(r, t) = n(r, t)/n_t$ the local proportion of the crystallized droplets, (3) becomes:

$$\dot{q} = \rho_0 V h_{SL} n_t\, d\phi/dt. \tag{5}$$

According to equation (4) we have:

$$\frac{d\phi}{dt} = \mathcal{J}(T(r,t))(1-\phi(r,t)). \tag{6}$$

As mentioned above we do not observe convective movements inside the emulsion. We only must resolve the conduction equation but, with a volumetric heat source $\dot{q}$ given by equations (5) and (6).

Taking into account equations (5) and (6), knowing that $n_t = (\rho P)/(\rho_0 V)$, (2) becomes:

$$\rho c \frac{\partial T(r,t)}{\partial t} = \nabla(k \nabla T(r,t)) + \rho P h_{SL} \mathcal{J}(T(r,t))(1-\phi(r,t)). \tag{7}$$

Equations (6) and (7) form a system where the unknowns are $T(r, t)$ and $\phi(r, t)$. These equations are non linear because of the function $\mathcal{J}(T(r, t))$ (see Fig. 1).

The boundaries conditions are classical:

for $r = 0$,

$$\left(\frac{\partial T}{\partial r}\right)_0 = 0 \tag{8}$$

for $r = R_0$,

$$-k\left(\frac{\partial T}{\partial r}\right)_{R_0} = h^{ext}(T(R_0,t) - T_\infty(t)) \tag{9}$$

where k is the thermal conductivity of the emulsion, h^{ext} an exchange coefficient between the emulsion and the bath to globally take into account the exchanges through the metallic tube and a part of the bath [10] and $T_\infty(t)$ is the imposed temperature of the bath. We have chosen, for the bath, either a full cooling with a linear variation such as:

$$T_\infty(t) = \beta t + cte \quad (\beta < 0) \tag{10}$$

or the same cooling but limited at a temperature T_l followed by a stabilization at this temperature afterwards.

For the initial conditions, we have chosen, as for

the experiments, a stabilized temperature for the cell. At $t = 0$ all the temperatures are the same:

$$T(r,0) = T_0. \tag{11}$$

As mentioned the function $\mathcal{J}(T)$ has been obtained by preliminary DSC experiments (see Fig. 1). Because of its definition, the coefficient h^{ext} cannot be measured. We have chosen a value compatible with the experimental results. The values of a, k or c are those determined at the ambient temperature. c and h_{SL} have been determined by DSC experiments.

If the values of ρ, c and k were constant, equation (7) would transform into:

$$\frac{\partial T(r,t)}{\partial t} = a\left(\frac{\partial^2 T(r,t)}{\partial r^2} + \frac{1}{r}\frac{\partial T(r,t)}{\partial r}\right) + bP\mathcal{J}(T(r,t))(1-\phi(r,t)) \tag{12}$$

where $a = k/\rho c$ is the diffusivity and $b = h_{SL}/c$.

The other equations are the same as equations (6), (8), (9), (10) or (11).

A preliminary study has shown the existence and the unicity of the solutions of the system of equations (6) and (12) [11].

In this case, it would be interesting to present dimensionless equations with the classical dimensionless variables:

$$\bar{t} = \frac{a}{R_0^2}t, \quad \bar{r} = \frac{r}{R_0}, \quad \theta = \frac{T-T_r}{T_0-T_r}. \tag{13}$$

We notice that it is not practical to choose a reference temperature T_r equal to the melting temperature T_F as it is often made in the literature because T_0 could be very near T_F and the undercooling important. We have chosen that θ could vary from 1 or 2 to -1 or -2. So, we have arbitrarily chosen T_r near the temperature where $\mathcal{J}(T)$ becomes different from zero and sharply increases. In this case, the crystallizations are detected for a value of θ around 0.

With these variables equations (12) and (6) become:

$$\frac{\partial\theta}{\partial\bar{t}} = \frac{\partial^2\theta}{\partial\bar{r}^2} + \frac{1}{\bar{r}}\frac{\partial\theta}{\partial\bar{r}} - \frac{P}{Ste}\mathcal{J}'(\theta)(1-\phi) \tag{14}$$

$$\frac{d\phi}{d\bar{t}} = \mathcal{J}'(\theta)(1-\phi) \tag{15}$$

where

$$Ste = \frac{c(T_0-T_r)}{h_{SL}}$$

is the Stefan number and $\mathcal{J}'(\theta)$ the dimensionless nucleation rate is

$$\mathcal{J}'(\theta) = \frac{R_0^2}{a}\mathcal{J}(T_r+\theta(T_0-T_r)).$$

The boundaries conditions would be:

$$\left(\frac{\partial\theta}{\partial\bar{r}}\right)_{\bar{r}=0} = 0 \tag{16}$$

$$\left(\frac{\partial\theta}{\partial\bar{r}}\right)_{\bar{r}=1} = Bi^{ext}[\theta_\infty - \theta(1,\bar{t})] \tag{17}$$

with

$$\theta_\infty = \beta'\bar{t} + 1 \tag{18}$$

where

$$\beta' = \frac{\beta}{T_0-T_r}\frac{R_0^2}{a}$$

the dimensionless cooling rate, and

$$Bi^{ext} = \frac{h^{ext}R_0}{k}$$

the external Biot number.

We can have a full cooling or a cooling limited at a temperature:

$$\theta_i = \frac{T_i-T_r}{T_0-T_r}.$$

The initial conditions are:

$$\text{for} \quad \bar{t} = 0 \quad \theta = 1. \tag{19}$$

We have already noticed the function $\mathcal{J}(T)$ is not linear. So, the dimensionless function $\mathcal{J}'(\theta)$ is not universal and the results described below are not universal. At a pinch it would be possible to analyse the relative influence of the parameters but the quantitative results could not be applied to different substances.

In fact, to have an accurate comparison between the model and the experimental results the above assumption is not adequate. In particular, even the variation of k and c is small with the temperature and we must take into account the notable difference for these values due to the fact that the disperse phase is liquid or solid. So, k or c depend mainly on ϕ the fraction of droplets already crystallized. We have already mentioned that the variation of ρ is negligible.

To simplify the problem, we assume, as it is predicted with a good approximation by different mixing laws [11], that k and c are linear functions of ϕ. We have:

$$k = k_L + (k_S - k_L)\phi(r,t) \tag{20}$$

and

$$c = c_L + (c_S - c_L)\phi(r,t) \tag{21}$$

where k_L and c_L are the heat conductivity and the specific heat of the emulsion when the dispersed phase is liquid and k_S and c_S the corresponding values when the dispersed phase is solid.

The heat conductivity and the specific heat are not constant, therefore finding non-dimensional variables is impossible. Moreover, the function $\mathcal{J}'(0)$ is not

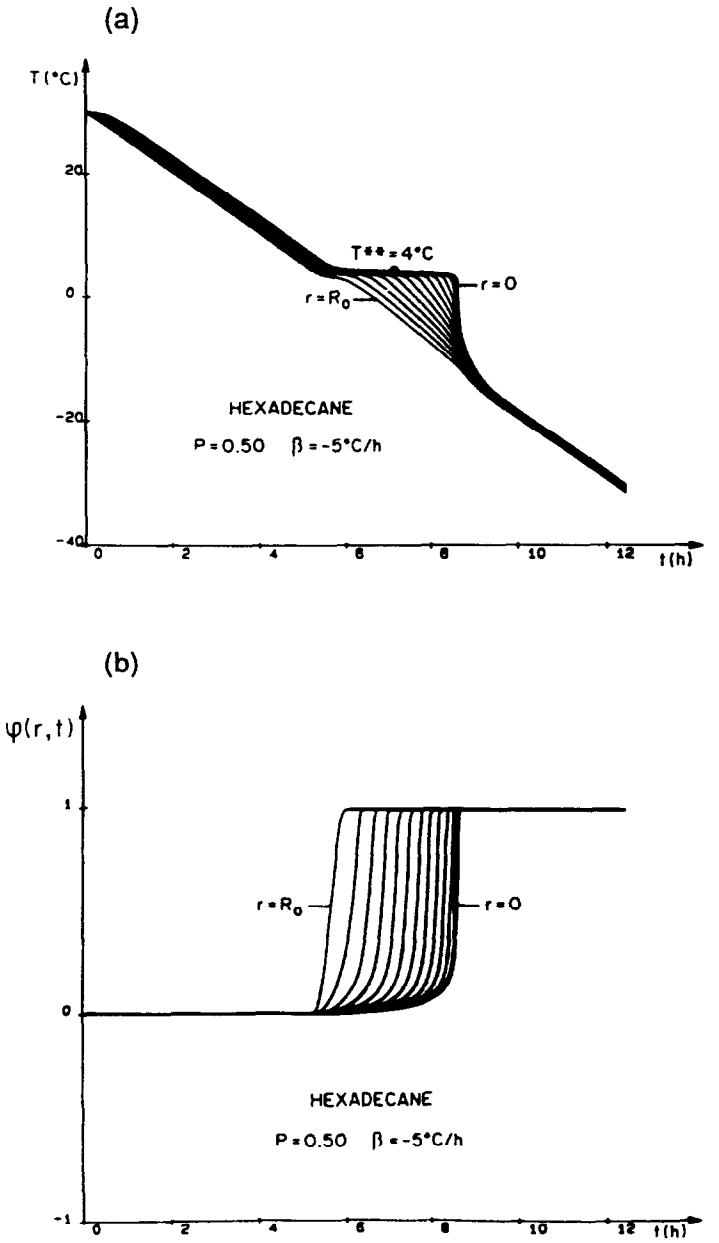

FIG. 6. (a) Calculated temperatures $T(r, t)$ at different radii from $r = 0$ to $r = R_0$ (step of 2.5 mm), vs time for a hexadecane emulsion cooled at $\beta = -5°C\ h^{-1}$ and (b) corresponding calculated proportions of crystallized droplets $\phi(r, t)$.

linear. So, we have kept the variables with their dimensions using equation (7) instead of equation (14).

The equations (6) and (7) taking into account the boundaries conditions (8)–(10) and the initial conditions (11), are solved by an explicit finite differences method.

As we have only one space variable, the grid consists of dividing the radius R_0 in M intervals with a length of Δr. The nodes, are located by $r = (m-1)\Delta r$ with $1 \leqslant m \leqslant M$. The interval of time being Δt, the time is such as $t = i\Delta t$. So, the energy equation (7) is:

$$\rho c(\phi_m^i)\frac{T_m^{i+1} - T_m^i}{\Delta t} = \frac{k(\phi_m^i)}{(\Delta r)^2}\left[\left(1 - \frac{1}{2(m-1)}\right)(T_{m-1}^i - T_m^i) + \left(1 + \frac{1}{2(m-1)}\right)(T_{m+1}^i - T_m^i)\right] + \rho h_{SL} P \mathcal{J}(T_m^i)(1 - \phi_m^i)$$

for $2 \leqslant m \leqslant M-1$.

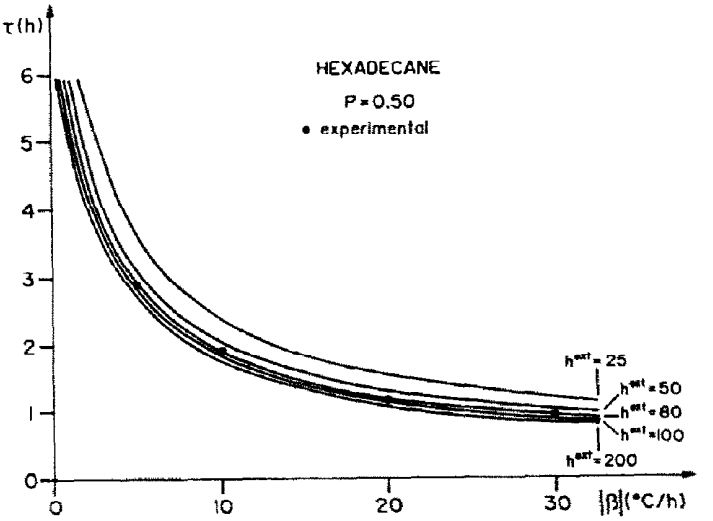

FIG. 7. Calculated values of τ for different values of the cooling rate β and different values of h^{ext} and comparison with the experiments.

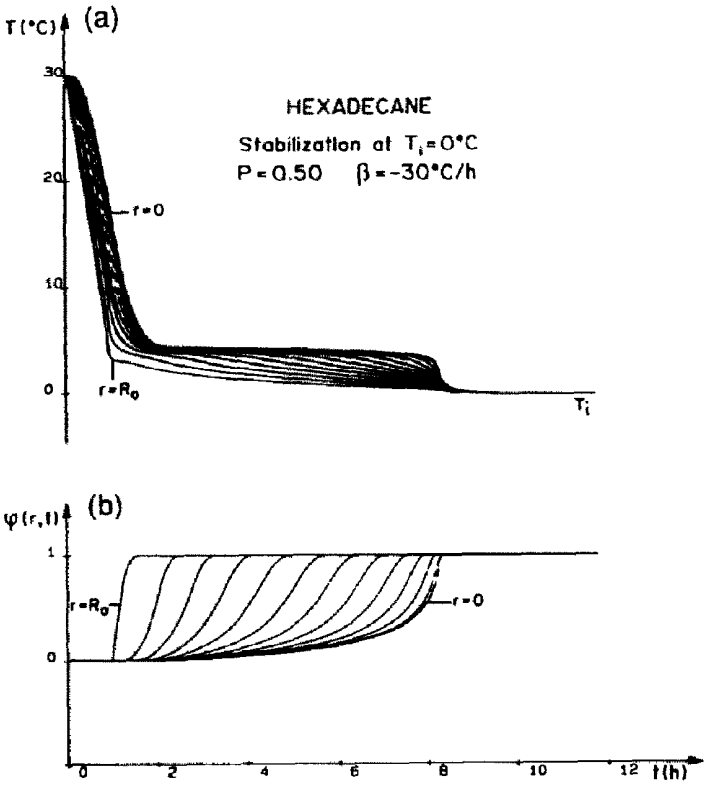

FIG. 8. (a) Calculated temperatures of the axis vs time for a hexadecane emulsion for coolings at $\beta = -30°C\ h^{-1}$ down to $T_i = 0°C$ and corresponding calculated values of $\phi(r, t)$ for different radii vs time.

Table 2. Experimental and calculated values of τ (h) for two mass fractions P of hexadecane.

P	Experimental	Model
0.50	1.10	1.19
0.25	0.90	0.85

For $m = 1$ ($r = 0$), equation (8) becomes:

$$\rho c(\phi_1^i)\frac{T_2^{i+1}-T_1^i}{\Delta t} = 4\frac{k(\phi_1^i)}{(\Delta r)^2}(T_2^i - T_1^i) + \rho h_{SL} P \mathcal{J}(T_1^i)(1-\phi_1^i)$$

and for $m = M$ ($r = R_0$), (9) becomes:

$$\rho c(\phi_M^i)\frac{T_M^{i+1}-T_M^i}{\Delta t} = \frac{k(\phi_M^i)}{(\Delta r)^2}\left(1-\frac{1}{2(M-1)}\right) \times (T_{M-1}^i - T_M^i) + \left(1-\frac{1}{2(M-1)}\right)\frac{h^{ext}}{\Delta r}(T_\infty^i - T_M^i) + \rho h_{SL} P \mathcal{J}(T_M^i)(1-\phi_M^i)$$

where $T_\infty^i = \beta i \Delta t + T_0$ after equation (10).

For all nodes, equation (6) is written as:

$$\frac{\phi_m^{i+1}-\phi_m^i}{\Delta t} = \mathcal{J}(T_m^i)(1-\phi_m^i) \quad m = 1, \ldots, M.$$

On Fig. 6(a), we have the calculated curves for a hexadecane emulsion ($P = 0.5$, $h_{SL} = 58$ cal g^{-1}, $k_L = 0.27$ W m^{-1} K^{-1}, $c_L = 2590$ J kg^{-1} K^{-1}, $k_S = 0.50$ W m^{-1} K^{-1}, $c_S = 2215$ J kg^{-1} K^{-1}, $\beta = -5$°C h^{-1}). The value of h^{ext} cannot be measured and is an adjustable constant. The value $h^{ext} = 80$ W m^{-2} K^{-1} has been chosen because, as we will see, studying the influence of different parameters, it is a value compatible with all our results.

In Fig. 6(a), we see that the shapes of the curves are identical with the experimental ones given in Fig. 3 and this fact confirms the validity of our model.

More information is given by the model if we plot the values of $\phi(r, t)$, the fraction of crystallized droplets. As indicated in Fig. 6(b), giving for each value of r the function $\phi(r, t)$ vs time and comparing with the corresponding curves on Fig. 6(a), we see that the proportion of crystallized droplets is very small when the temperature is stabilized around T^{**}. $\phi(r, t)$ increases sharply only at the end of the temperature plateau and the temperature decreases only just after the crystallizations of all droplets.

We conclude that, for a full cooling, the region where the droplets are crystallizing corresponds to a narrow radius range which slowly moves from $r = R_0$ to the axis.

To compare the results when the different parameters are changed, because of the same general shape of the curves and because T^{**} varies very little, it is sufficient to analyse the variation of τ the duration of the axis temperature plateau.

Influence of the cooling rate β

In Fig. 7 we have plotted curves giving the values of τ vs $-\beta$ (β is negative) calculated according to the model. The experimental values are conformable to the curve for $h^{ext} = 80$ W m^{-2} K^{-1}. In fact for $h^{ext} \geqslant 50$ W m^{-2} K^{-1} when the heat transfer is assumed sufficient, τ is only slightly dependent on the value of h^{ext}. The kinetics of the global effect depends only on the heat transfers inside the emulsion.

Figure 7 indicates that τ decreases when $-\beta$ increases but τ is not proportional to $-\beta$.

Influence of the mass fraction P

It is difficult to resolve the model for different values of the mass fraction P because the characteristic parameters k, c or ρ of the dispersed system depend on it [12]. For the dispersion of hexadecane, it is not possible to have a microemulsion for all values of the mass fraction and, if it is possible to have a microemulsion for $P = 0.50$, for certain smaller values of P, we are only able to make an emulsion.

So, we have only studied the mass fractions 0.50 and 0.25 whose parameters have been determined [12]. In Table 2 we compare the experimental and theoretical results for τ (full cooling at $\beta = -20$°C h^{-1}). The values are in good agreement.

Influence on the lower temperature T_i

The cooling is limited to a temperature T_i and stabilized at this temperature afterwards. When T_i is sufficiently low we have a full cooling which corresponds to the above results. But when T_i is higher, close to the plateau temperature T^{**} (indeed $T_i < T^{**}$), the results are different. Although we observe a plateau at the same temperature, the value of τ is considerably increased, as indicated in Fig. 8(a), for the experimental and theoretical curves for the axis.

In Fig. 8(b), we have the corresponding curves of the proportions of crystallized droplets $\phi(r, t)$ vs time for different radii. We conclude that the moving region where the droplets are crystallizing is broader than with a full cooling.

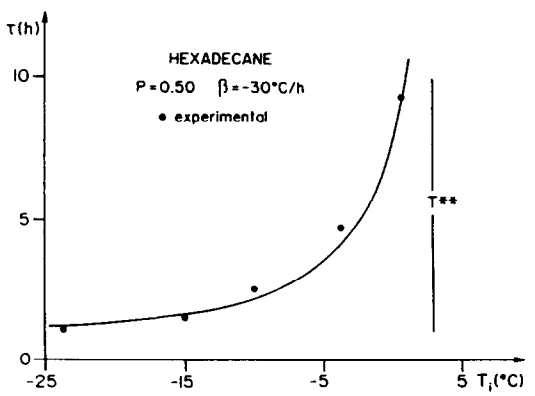

FIG. 9. Calculated and experimental values of τ vs T_i.

In Fig. 9 we compare for different values of T_i the experimental values of τ and the calculated values. In spite of the difficulty to have the quasi perfect stability of temperature for a long time, the experimental and calculated values are in accordance.

5. CONCLUSION

In this first part, we have presented experimental results concerning the study of heat transfers inside a steadily cooled emulsion when the dispersed phase crystallizes.

The model presented is based on the resolution of the energy equation with a heat source depending on the probability of crystallization given by the nucleation theories. We observe a good agreement with the experimental results. In particular we have observed a stabilization of the temperature in the axis region of the cell during a lapse of time which:

- decreases when the mass fraction decreases;
- increases when the cooling rate decreases;
- largely increases when the final temperature increases.

REFERENCES

1. J. P. Dumas, M. Strub, M. Krichi, F. Broto and Y. Zeraouli, Experiments on heat transfer during melting or freezing of droplets within an emulsion, *Eurotherm Seminar 5*, Compiegne, France (1988).
2. J. P. Dumas, M. Strub and F. Broto, Heat transfer during the freezing of undercooled liquids dispersed within an emulsion, *9th International Heat Transfer Conference*, Jerusalem, Israel, 19–24 August (1990).
3. D. Clausse, J. P. Dumas, P. H. E. Meijer and F. Broto, Phases transformations in emulsions: Part I—Effects of thermal treatments on nucleation phenomena, *J. Dispersion Sci. Technol.* **8**(1), 1–28 (1987). J. P. Dumas, F. Tounsi and L. Babin, Phases transformations in emulsions: Part II—Polymorphism for organic substances, *J. Dispersion Sci. Technol.* **8**(1), 29–54 (1987).
4. J. H. Perepezko and D. H. Rasmussen, Solidification of highly undercooled liquid metals and alloys, *Proc. 17th Aerospace Sci. Meet.*, New Orleans (1979).
5. M. Aguerd, D. Clausse and L. Babin, Heterogeneous nucleation of ice by AgI in water dispersed within emulsions, *Cryo-Letters* **3**, 164–171 (1982).
6. L. Babin, D. Clausse, I. Sifrini, F. Broto et D. Clausse, Nucléation par le Borax du Sulfate de Sodium dispersé. Application au Stockage Thermique, *J. Physique* **39**, 359 (1978).
7. F. Broto and D. Clausse, A study of the freezing of supercooled water dispersed within emulsions by differential scanning calorimetry, *J. Phys. C: Solid State Phys.* **9**, 4251–4257 (1976).
8. D. Turnbull, Phases change. In *Solid State Physics*, Vol. 2, pp. 226–306. Academic Press, New York (1956).
9. Y. Zeraouli, Etude thermique des transformations des emulsions concentrées. Application à la calorimètrie à balayage, Thesis, Pau (1991).
10. M. Krichi, Etude des transferts thermiques dans des systèmes dispersés subissant des transformations de phases, Thesis, Pau (1992).
11. G. Vallet, Modélisation mathématique de processus thermiques des changements de phases dans une émulsion, *XXIII Congrés National d'Analyse Numérique*, Royan, France, 27–31 May (1991).
12. R. Kenneth, E. C. Foster and B. L. Jonathan, Transport properties of polymer solutions. A comparative approach, *Biophy. J. Biophys. Soc.* **45**, 975–984 (1984).